Computer-Aided Design and Applications

http://www.cadanda.com

Degree Elevation and Reduction of Periodic Surfaces

Yan Wang

University of Central Florida, wangyan@mail.ucf.edu

ABSTRACT

Recently we developed a periodic surface model to assist the construction of nano structures parametrically for computer-aided nano-design. In this paper, we study the properties of periodic surfaces for degree elevation and reduction. Degree elevation approaches are developed to incrementally increase shape complexities, including native, variational, and boundary constrained elevations. A generic degree reduction operation is defined for surface approximation based on an algebraic distance. The goal is to enhance the flexibility of the periodic surface model and allow for multi-resolution representation.

Keywords: periodic surface; implicit surface; surface approximation; computer-aided nano-design.
DOI: 10.3722/cadaps.2008.841-854

1. INTRODUCTION

Computer-aided nano-design (CAND) is an extension of computer based engineering design traditionally at bulk scales to nano scales. Enabling efficient structural description is one of the key research issues in CAND. Traditional boundary-based parametric solid modeling methods for engineering design do not support efficient construction of complex nano-scale geometries, such as super-porous structures and crystal packing. Visualization methods such as models of space-filled, wireframe, stick, ball-and-stick, ribbon and solvent-accessible surface do not support parametric construction and modification of molecular structures. Providing engineers and scientists efficient and easy-to-use tools to create structures that are reasonably close to optimal conformations with the minimum energy is highly desirable to improve the efficiency of simulation in material design. Expanding the horizon of available shapes for design engineers for nano-scale geometries is a new task in developing CAND tools.

With the observation that hyperbolic surfaces exist in nature ubiquitously and periodic features are common in condensed materials, we recently proposed an implicit surface modeling approach, periodic surface (PS), to represent geometric structures in nano scales [1, 2]. Periodic surfaces are either loci or foci. Loci surfaces are fictional continuous surfaces that pass through discrete particles in 3D space, whereas foci surfaces can be looked as isosurfaces of potential or density in which discrete particles are enclosed. The surface model allows for parametric construction from atomic scale to meso scale. Reconstruction of loci surfaces from crystals was also studied [3].

In this paper, we study the properties of degree elevation and reduction for periodic surfaces, which are two basic mechanisms to control the complexity of periodic surfaces and enable multi-resolution representation. In the remainder of the paper, Section 2 gives an overview of related work and the periodic surface model. Section 3 describes three approaches of degree elevation. And Section 4 presents a generic degree reduction method based on an algebraic distance measurement.

2. BACKGROUND

2.1 Implicit Surface Modeling

Implicit surfaces [4] are not as widely used as parametric surfaces in interactive modeling environment, largely due to the lack of intuitive shape manipulation and control. Yet, implicit surface modeling has some advantages such as straightforward ray tracing and closure of Boolean operations. Research in implicit surface modeling include "blobby model" based on the Gaussian kernel [5, 6, 7] and polynomials [8]. Topics such as implicitization [9, 10, 11, 12, 13], blending [14, 15, 16, 17, 18], interpolation [19, 20], control [21, 22], curvature formulation [23, 24, 25], as well as polygonization [26, 27, 28] and direct ray tracing [29, 30] have been studied.

2.2 Molecular Surface Modeling

For visualization purpose, there has been some research on molecular surface modeling to visualize molecular structures [31]. Lee and Richards [32] first introduced solvent-accessible surface, the locus of a probe rolling over Van der Waals surface, to represent boundary of molecules. Connolly [33] presented an analytical method to calculate the surface. Recently, Carson [34] represented molecular surfaces with B-spline wavelet. Edelsbrunner [35] described molecules with implicit-form skin surfaces. Bajaj et al. [36] represented solvent accessible surfaces by NURBS (non-uniform rational B-spline). Au and Woo [37] studied the topological changes of macromolecules during folding with the aid of ribbons. Ryu et al. [38] constructed NURBS molecular surfaces by the aid of Euclidean Voronoi diagrams. Zhang et al. [39] constructed implicit solvation surfaces from the Gaussian kernel. These research efforts concentrate on visualization of molecules, whereas construction support of molecular structures for design purpose is not considered.

2.3 Periodic Surface

We recently proposed a periodic surface (PS) model to represent nano-scale geometries. It has the implicit form

$$\psi(\mathbf{r}) = \sum_{l=1}^{L}\sum_{m=1}^{M} \mu_{lm} \cos\left(2\pi\kappa_l(\mathbf{p}_m^T \cdot \mathbf{r})\right) = 0 \tag{2.1}$$

where κ_l is the *scale parameter*, $\mathbf{p}_m = [a_m, b_m, c_m, \theta_m]^T$ is a *basis vector*, such as one of

$$\{\mathbf{e}_0, \mathbf{e}_1, \mathbf{e}_2, \mathbf{e}_3, \mathbf{e}_4, \mathbf{e}_5, \mathbf{e}_6, \mathbf{e}_7, \mathbf{e}_8, \mathbf{e}_9, \mathbf{e}_{10}, \mathbf{e}_{11}, \mathbf{e}_{12}, \mathbf{e}_{13}, \ldots\} =$$

$$\left\{ \begin{bmatrix}0\\0\\0\\1\end{bmatrix} \begin{bmatrix}1\\0\\0\\1\end{bmatrix} \begin{bmatrix}0\\1\\0\\1\end{bmatrix} \begin{bmatrix}0\\0\\1\\1\end{bmatrix} \begin{bmatrix}1\\1\\0\\1\end{bmatrix} \begin{bmatrix}1\\0\\1\\1\end{bmatrix} \begin{bmatrix}0\\1\\1\\1\end{bmatrix} \begin{bmatrix}1\\1\\1\\1\end{bmatrix} \begin{bmatrix}1\\-1\\0\\1\end{bmatrix} \begin{bmatrix}-1\\0\\1\\1\end{bmatrix} \begin{bmatrix}0\\1\\-1\\1\end{bmatrix} \begin{bmatrix}1\\-1\\1\\1\end{bmatrix} \begin{bmatrix}-1\\1\\1\\1\end{bmatrix} \begin{bmatrix}1\\1\\-1\\1\end{bmatrix} \ldots \right\} \tag{2.2}$$

which represents a *basis plane* in the 3-space $\mathbb{E}^3$, $\mathbf{r} = [x, y, z, w]^T$ is the location vector with homogeneous coordinates, and μ_{lm} is the *periodic moment*. We assume $w = 1$ if not explicitly specified. The *degree* of $\psi(\mathbf{r})$ in Eqn.(2.1) is defined as the number of unique periodic vectors in $\{\mathbf{p}_m\}$. The *scale* of $\psi(\mathbf{r})$ is defined as the number of unique scale parameters in $\{\kappa_l\}$. In this paper, we assume scale parameters are natural numbers ($\kappa_l \in \mathbb{N}$).

Fig. 1 lists some examples of PS models. Triply periodic minimal surfaces, such as P-, D-, G-, and I-WP cubic morphologies that are frequently referred to in chemistry and polymer literature, can be adequately approximated. Besides the cubic phase, other mesophase structures such as spherical micelles, lamellar, rodlike hexagonal phases can also be modeled.

With the aid of continuous PS models, discrete crystals can be constructed by operations such as intersection and modulation. Basis vectors play an important role in model construction and interactive manipulation. As illustrated in Fig. 2, each basis vector represents a 2D subspaces in $\mathbb{E}^3$. We call $d_m = \hat{\mathbf{p}}_m^T \cdot \mathbf{r} = \mathbf{p}_m^T \cdot \mathbf{r} / \|\mathbf{p}_m\|$ the *projective distance* between the origin and the subspace where $\mathbf{r}$ resides with respect to the basis plane $\mathbf{p}_m$. We call $\mathbf{e}_0 = [0, 0, 0, 1]^T$ in Eqn.(2.2) the *ideal plane* in which the corresponding projective distance does not depend on the Euclidean position of $\mathbf{r}$.

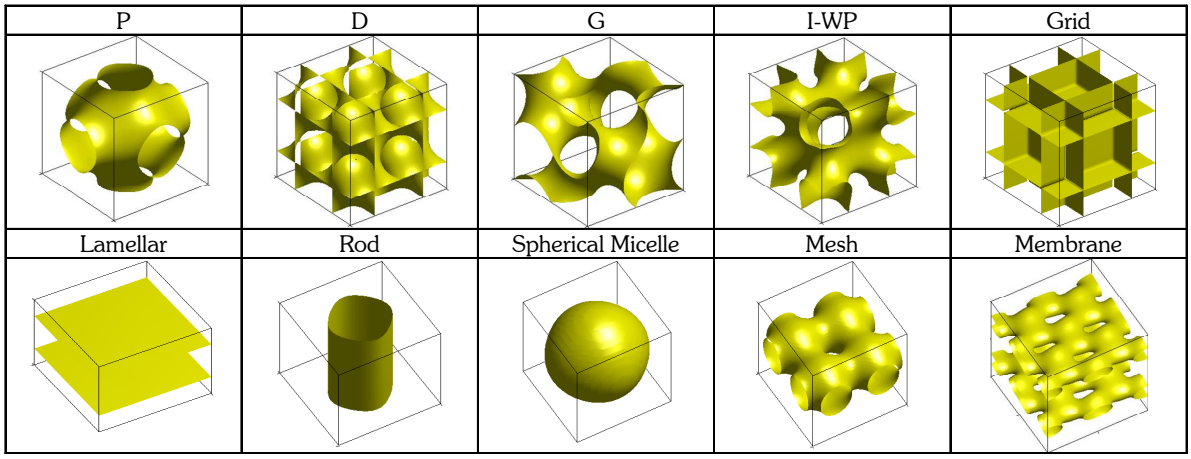

Fig. 1: Periodic surface models of cubic phase and mesophase structures [2].

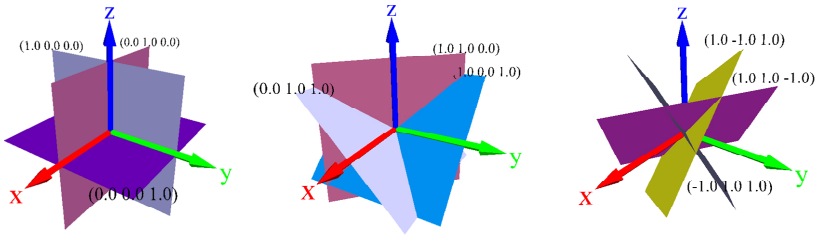

(a) basis vectors form discrete 2D subspaces

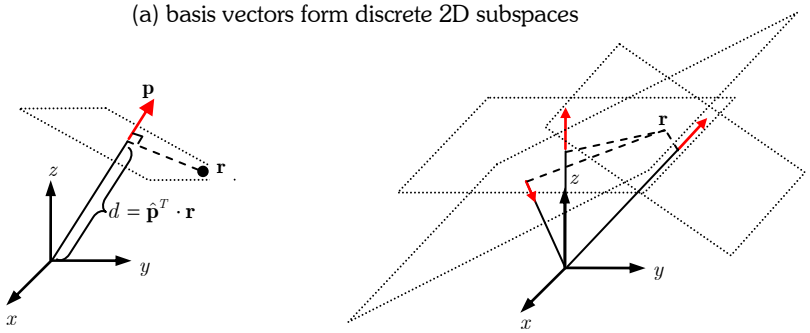

(b) projective distances between origin and basis planes

Fig. 2: Discrete subspaces corresponding to basis planes.

A volume domain $\mathbb{D} = [\underline{x}, \overline{x}] \times [\underline{y}, \overline{y}] \times [\underline{z}, \overline{z}] \times 1 \subseteq \mathbb{R}^4$ is called *complete* for a periodic surface $\psi(\mathbf{r})$ if

$$\iiint_{\mathbb{D}} \psi(\mathbf{r}) d\mathbf{r} = 0 \Leftrightarrow \forall \mathbf{r} \in \mathbb{D}, \forall n \in \mathbb{N}(n \neq 0), \psi(\mathbf{r} + n\mathbf{R}) = \psi(\mathbf{r}) \tag{2.3}$$

where $\mathbf{R} = [\overline{x} - \underline{x}, \overline{y} - \underline{y}, \overline{z} - \underline{z}, 0]^T \neq \mathbf{0}$ is the *range* of $\mathbb{D}$. If the number of period within $\mathbb{D}$ is 1, that is, for $\forall \mathbb{D}' \subset \mathbb{D}\ (\mathbb{D}' \neq \varnothing)$, $\iiint_{\mathbb{D}'} \psi(\mathbf{r}) d\mathbf{r} \neq 0$, then $\mathbb{D}$ is called a *minimally complete* domain for $\psi(\mathbf{r})$. In general, the inner product of two periodic surfaces in a domain $\mathbb{D}$ is defined as

$$\langle \psi_1(\mathbf{r}), \psi_2(\mathbf{r}) \rangle := \iiint_{\mathbb{D}} \psi_1(\mathbf{r}) \psi_2(\mathbf{r}) d\mathbf{r} \tag{2.4}$$

Two periodic basis vectors $\mathbf{p}_1$ and $\mathbf{p}_2$ are called *orthogonal* at scales κ_1 and κ_2 respectively in a domain $\mathbb{D}$ if the corresponding periodic basis functions $\cos\left(2\pi\kappa_1(\mathbf{p}_1^T\cdot\mathbf{r})\right)$ and $\cos\left(2\pi\kappa_2(\mathbf{p}_2^T\cdot\mathbf{r})\right)$ have the relation

$$\left\langle\cos\left(2\pi\kappa_1(\mathbf{p}_1^T\cdot\mathbf{r})\right),\cos\left(2\pi\kappa_2(\mathbf{p}_2^T\cdot\mathbf{r})\right)\right\rangle=\iiint_{\mathbb{D}}\cos\left(2\pi\kappa_1(\mathbf{p}_1^T\cdot\mathbf{r})\right)\cos\left(2\pi\kappa_2(\mathbf{p}_2^T\cdot\mathbf{r})\right)d\mathbf{r}=0 \tag{2.5}$$

Notice that orthogonality of basis vectors is scale and domain dependent. Two periodic surfaces $\psi_1(\mathbf{r})$ and $\psi_2(\mathbf{r})$ are called *orthogonal* if there exists a domain $\mathbb{D}\neq\varnothing$ such that

$$\langle\psi_1,\psi_2\rangle=\iiint_{\mathbb{D}}\psi_1(\mathbf{r})\psi_2(\mathbf{r})d\mathbf{r}=0 \tag{2.6}$$

3. DEGREE ELEVATION

Degree elevation allows us to incrementally increase the complexity of models. Three approaches of degree elevation for periodic surfaces are studied here. They include the scale-independent native degree elevation, scale-dependent variational degree elevation, and constrained degree elevation with boundary conditions of continuity.

3.1 Native Degree Elevation

Because of the orthogonality of periodic basis functions, the native degree elevation of Eqn.(2.1) is to simply add new basis vectors with the corresponding moments as zeros. That is,

$$\psi'(\mathbf{r})=\sum_{l=1}^{L}\sum_{m=1}^{M+V}\mu_{lm}\cos\left(2\pi\kappa_l(\mathbf{p}_m^T\cdot\mathbf{r})\right)=0 \tag{3.1}$$

where $\mu_{lm}=0$ for all $l=1,\ldots,L$ and $m=M+1,\ldots,M+V$.

Example 1. Zeolites are known as molecular sieves that have porous structures of molecular sizes. This allows small molecules such as water to pass through layers of sieves while bigger molecules are filtered out. Zeolites are widely applied for purification and separation as detergent, catalyst, and others. Fig. 3 shows a loci PS model for one type of zeolites, Faujasite crystal.

$$\begin{aligned}\psi(x,y,z)=&-0.50992-0.0098336\cos(2\pi x)\\&-0.0098336\cos(2\pi y)-0.0098336\cos(2\pi z)\\&-0.0042982\cos(2\pi(x+y))-0.0042982\cos(2\pi(x+z))\\&-0.0042982\cos(2\pi(y+z))-0.015304\cos(2\pi(x-y))\\&-0.015304\cos(2\pi(z-x))-0.015304\cos(2\pi(y-z))\\&-0.45206\cos(2\pi(x+y+z))+0.42213\cos(2\pi(x-y+z))\\&+0.42213\cos(2\pi(y+z-x))+0.42213\cos(2\pi(x+y-z))\\=&\,0\end{aligned}$$

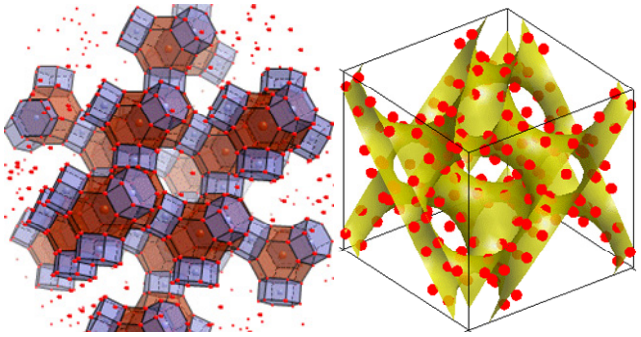

(a) Faujasite crystal. Each tetradecahedron encloses a **Fe**, each hexagonal prism encloses an **Al**, and each vertex of the polygons represents a **Si**.

(b) Loci PS model of **Si** in Faujasite

Fig. 3: Loci PS model of Faujasite crystal.

If 1/8 of the model in Fig. 3(b) is considered, we can have a zoom-in view of the model as in Fig. 4(a). When more detailed controls during the design process are needed so that the positions of atoms can be fine-tuned, the degree elevation operation provides the needs. We may introduce three more basis vectors with the corresponding moments as zeros. Modifying the moments further we can create a different design, such as the new surface model $\psi'(\mathbf{r})$ in Fig. 4(b).

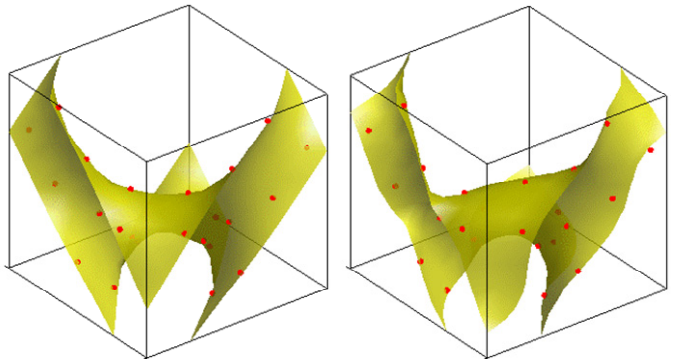

$$\psi'(x,y,z) = \psi(x,y,z) - 0.1\cos(2\pi(x-3y-z)) + 0.1\cos(2\pi(y-x-3z)) - 0.1\cos(2\pi(z-3x-y)) = 0$$

(a) Original loci PS model $\psi(\mathbf{r})$ (b) An example of the elevated PS model $\psi'(\mathbf{r})$ to support detailed modifications

Fig. 4: An example of degree elevation to support fine-tuned modification of the Faujasite PS model.

3.2 Variational Degree Elevation

There exists no general scale-independent degree elevation such that $\forall \mathbf{r} \in \mathbb{P}^3$

$$\sum_{m=1}^{M} \mu_{lm} \cos\left(2\pi\kappa(\mathbf{p}_m^T \cdot \mathbf{r})\right) = \sum_{n=1}^{N} \mu'_{ln} \cos\left(2\pi\kappa(\mathbf{p}'^T_n \cdot \mathbf{r})\right) \tag{3.2}$$

where $\{\mathbf{p}_m\} \neq \{\mathbf{p}'_n\}$, $\mu_{lm} \neq 0$ and $\mu'_{ln} \neq 0$ for all l,m,n, and $M,N < \infty$ at some scale κ.

Although there is no general non-native scale-independent degree elevation scheme, we can have an approximated variational degree elevation that is scale-dependent. For some small $\Delta\mathbf{p}_m$'s,

$$\begin{aligned}
&\sum_{l=1}^{L}\sum_{m=1}^{M} \mu_{lm} \cos\left(2\pi\kappa_l((\mathbf{p}_m^T + \Delta\mathbf{p}_m{}^T) \cdot \mathbf{r})\right) \approx \\
&\sum_{l=1}^{L}\sum_{m=1}^{M} \mu_{lm} \left[\cos\left(2\pi\kappa_l(\mathbf{p}_m^T \cdot \mathbf{r})\right) - \cos\left(2\pi\kappa_l(\mathbf{p}_m^T \cdot \mathbf{r} - \frac{1}{4\kappa_l})\right)(2\pi\kappa_l \Delta\mathbf{p}_m{}^T \cdot \mathbf{r})\right] \\
&= \sum_{l=1}^{L}\sum_{m=1}^{M} \mu_{lm} \left[\cos\left(2\pi\kappa_l(\mathbf{p}_m^T \cdot \mathbf{r})\right) - \cos\left(2\pi\kappa_l(\mathbf{q}_{lm}^T \cdot \mathbf{r})\right)(2\pi\kappa_l \Delta\mathbf{p}_m{}^T \cdot \mathbf{r})\right]
\end{aligned} \tag{3.3}$$

where $\mathbf{q}_{lm} = (a_m, b_m, c_m, \theta_m - 1/(4\kappa_l w))$ is a scale-dependent translated $\mathbf{p}_m$. In a given domain $\mathbb{D}$, for any l and m, if we can find some small moments $\Delta\mu_{lm}$'s such that

$$\Delta\mu_{lm} = \max_{\forall \mathbf{r} \in \mathbb{D}} \left|\mu_{lm}(\Delta\mathbf{p}_m{}^T \cdot \mathbf{r})\right| \tag{3.4}$$

then the scale-dependent variational degree elevation is

$$\begin{aligned}
&\sum_{l=1}^{L}\sum_{m=1}^{M} \mu_{lm} \cos\left(2\pi\kappa_l(\mathbf{p}_m^T \cdot \mathbf{r})\right) \\
&\approx \sum_{l=1}^{L}\sum_{m=1}^{M} \mu_{lm} \cos\left(2\pi\kappa_l((\mathbf{p}_m^T + \Delta\mathbf{p}_m{}^T) \cdot \mathbf{r})\right) + \sum_{l=1}^{L}\sum_{m=1}^{M} 2\pi\kappa_l \Delta\mu_{lm} \cos\left(2\pi\kappa_l(\mathbf{q}_{lm}^T \cdot \mathbf{r})\right)
\end{aligned} \tag{3.5}$$

For a given domain $\mathbb{D}$, the largest projective distances occur at the vertices of $\mathbb{D}$. As illustrated in Fig. 5, the largest $\Delta\mathbf{p}_m{}^T \cdot \mathbf{r}$ in the 2D domain always occurs at the corner points. Thus the lower and upper bounds of $\Delta\mu_{lm}$'s can be easily estimated.

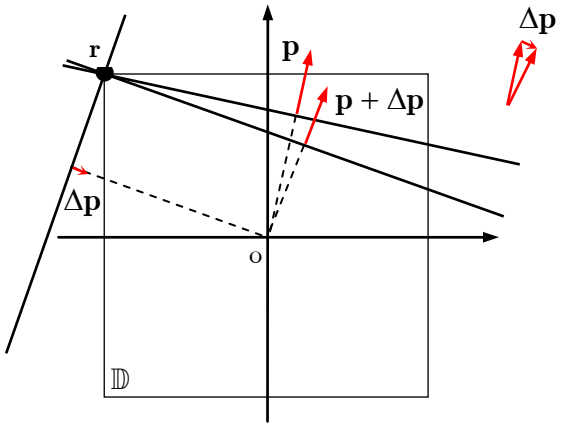

Fig. 5: The lower and upper bounds of $\Delta\mu_{lm}$ are estimated at the vertices of domains.

Example 2. P surfaces can be used to model cage-like structures, such as Sodalite minerals in Fig. 6(a). In the standard unit domain

$$\mathbb{D}_0 := \{(x,y,z,1) \mid 0 \le x \le 1; 0 \le y \le 1; 0 \le z \le 1\} \tag{3.6}$$

an example of variational degree elevation of a standard P surface with the scale parameter $\kappa = 1$ and moments $\mu_1 = \mu_2 = \mu_3 = 1$ can be obtained as follows. Basis vectors are $\mathbf{p}_1 = [1,0,0]^T$, $\mathbf{p}_2 = [0,1,0]^T$, and $\mathbf{p}_3 = [0,0,1]^T$. Suppose vector deviations are $\Delta\mathbf{p}_1 = [0.001,0,0]^T$, $\Delta\mathbf{p}_2 = [0.001,0.001,0]^T$, and $\Delta\mathbf{p}_3 = [0.001,0.001,0.001]^T$. It is easy to find $\Delta\mu_1 = 0.001$, $\Delta\mu_2 = 0.002$, and $\Delta\mu_3 = 0.003$. With different vector deviations $\Delta\mathbf{p}_j\,(j = 1,2,3)$, the original and elevated surfaces are compared in Fig. 6.

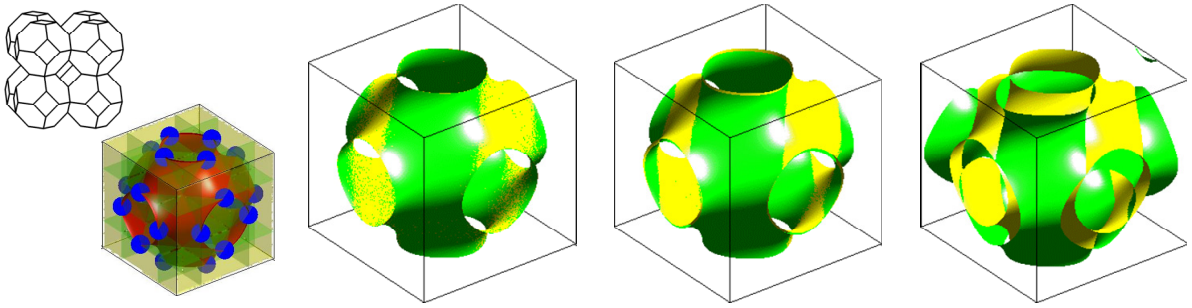

(a) P surface models Sodalite lattice of 14-sided cages. Vertices correspond to Si (Al) and edges represent Si-O-Si (Si-O-Al) bonds

(b) $\Delta\mathbf{p}_1 = [0.001,0,0]^T$, $\Delta\mathbf{p}_2 = [0.001,0.001,0]^T$, $\Delta\mathbf{p}_3 = [0.001,0.001,0.001]^T$

(c) $\Delta\mathbf{p}_1 = [0.01,0,0]^T$, $\Delta\mathbf{p}_2 = [0.01,0.01,0]^T$, $\Delta\mathbf{p}_3 = [0.01,0.01,0.01]^T$

(d) $\Delta\mathbf{p}_1 = [0.1,0,0]^T$, $\Delta\mathbf{p}_2 = [0.1,0.1,0]^T$, $\Delta\mathbf{p}_3 = [0.1,0.1,0.1]^T$

Fig. 6: Examples of variational degree elevation of P surface, where each of the yellow surfaces is the original P surface and each of the green surfaces is the elevated one.

Example 3. We apply variational degree elevation to the Faujasite crystal model in Fig. 3. The elevated surface $\psi''(\mathbf{r})$ is shown in Fig. 7(b).

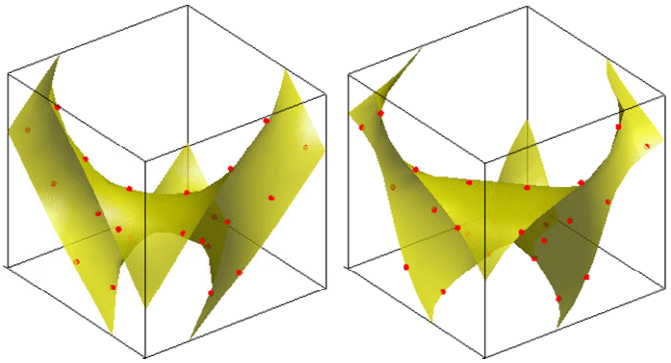

$$\psi''(x,y,z) = \psi(x,y,z) + 0.15\cos(2\pi(1.1x + y + z - 0.25)) + 0.15\cos(2\pi(1.1x - y + z - 0.25)) + 0.15\cos(2\pi(y + z - 1.1x - 0.25)) + 0.15\cos(2\pi(1.1x + y - z - 0.25)) = 0$$

(a) Original loci PS model $\psi(\mathbf{r})$ of Faujasite crystal

(b) The variationally elevated PS model $\psi''(\mathbf{r})$

Fig. 7: Variationally elevated surface model of the Faujasite crystal in Fig. 3.

Theorem 1. The variational degree elevation is an approximation with quadratic convergence.

Proof. For any l and m,

$$\begin{aligned}
Q_{lm} &= \mu_{lm}\cos\left(2\pi\kappa_l(\mathbf{p}_m^T\cdot\mathbf{r})\right) - \left[\mu_{lm}\cos\left(2\pi\kappa_l((\mathbf{p}_m^T + \Delta\mathbf{p}_m{}^T)\cdot\mathbf{r})\right) + 2\pi\kappa_l\mu_{lm}(\Delta\mathbf{p}_m{}^T\cdot\mathbf{r})\cos\left(2\pi\kappa_l(\mathbf{q}_m^T\cdot\mathbf{r})\right)\right] \\
&= \mu_{lm}\cos\left(2\pi\kappa_l(\mathbf{p}_m^T\cdot\mathbf{r})\right) - \mu_{lm}\cos\left(2\pi\kappa_l(\mathbf{p}_m^T\cdot\mathbf{r})\right)\cos\left(2\pi\kappa_l(\Delta\mathbf{p}_m{}^T\cdot\mathbf{r})\right) \\
&\quad + \mu_{lm}\sin\left(2\pi\kappa_l(\mathbf{p}_m^T\cdot\mathbf{r})\right)\sin\left(2\pi\kappa_l(\Delta\mathbf{p}_m{}^T\cdot\mathbf{r})\right) - 2\pi\kappa_l\mu_{lm}(\Delta\mathbf{p}_m{}^T\cdot\mathbf{r})\sin\left(2\pi\kappa_l(\mathbf{p}_m^T\cdot\mathbf{r})\right) \\
&= \mu_{lm}\cos\left(2\pi\kappa_l(\mathbf{p}_m^T\cdot\mathbf{r})\right)\left[1 - \cos\left(2\pi\kappa_l(\Delta\mathbf{p}_m{}^T\cdot\mathbf{r})\right)\right] + \mu_{lm}\sin\left(2\pi\kappa_l(\mathbf{p}_m^T\cdot\mathbf{r})\right)\left[\sin\left(2\pi\kappa_l(\Delta\mathbf{p}_m{}^T\cdot\mathbf{r})\right) - 2\pi\kappa_l\Delta\mathbf{p}_m{}^T\cdot\mathbf{r}\right]
\end{aligned}$$

Since $\cos(x) = 1 - \frac{x^2}{2!} + \frac{x^4}{4!} + O\left(x^6\right)$ and $\sin(x) = x - \frac{x^3}{3!} + \frac{x^5}{5!} + O\left(x^7\right)$ when $x \to 0$,

$$\begin{aligned}
Q_{lm} &= \mu_{lm}\cos\left(2\pi\kappa_l(\mathbf{p}_m^T\cdot\mathbf{r})\right)\left[\frac{(2\pi\kappa_l\Delta\mathbf{p}_m{}^T\cdot\mathbf{r})^2}{2!} + O\left((2\pi\kappa_l\Delta\mathbf{p}_m{}^T\cdot\mathbf{r})^4\right)\right] \\
&\quad + \mu_{lm}\sin\left(2\pi\kappa_l(\mathbf{p}_m^T\cdot\mathbf{r})\right)\left[\left((2\pi\kappa_l\Delta\mathbf{p}_m{}^T\cdot\mathbf{r}) - \frac{(2\pi\kappa_l\Delta\mathbf{p}_m{}^T\cdot\mathbf{r})^3}{3!}\right) - (2\pi\kappa_l\Delta\mathbf{p}_m{}^T\cdot\mathbf{r}) + O\left((2\pi\kappa_l\Delta\mathbf{p}_m{}^T\cdot\mathbf{r})^5\right)\right] \\
&= \mu_{lm}\left[\cos\left(2\pi\kappa_l(\mathbf{p}_m^T\cdot\mathbf{r})\right)\frac{(2\pi\kappa_l\Delta\mathbf{p}_m{}^T\cdot\mathbf{r})^2}{2!} - \sin\left(2\pi\kappa_l(\mathbf{p}_m^T\cdot\mathbf{r})\right)\frac{(2\pi\kappa_l\Delta\mathbf{p}_m{}^T\cdot\mathbf{r})^3}{3!}\right] + O\left((2\pi\kappa_l\Delta\mathbf{p}_m{}^T\cdot\mathbf{r})^4\right) \\
&= \mu_{lm}\cos\left(2\pi\kappa_l(\mathbf{p}_m^T\cdot\mathbf{r})\right)\frac{(2\pi\kappa_l\Delta\mathbf{p}_m{}^T\cdot\mathbf{r})^2}{2} + O\left((2\pi\kappa_l\Delta\mathbf{p}_m{}^T\cdot\mathbf{r})^3\right)
\end{aligned}$$

□

3.3 Constrained Degree Elevation

Complex nanostructures are expected to be assembled based on some basic building blocks. Piecewise construction is needed in the assembly process. To support piecewise construction of PS models, certain levels of surface continuity conditions may be required at the domain boundaries in degree elevation, which is called the constrained degree elevation process.

Theorem 2 ([19]). If implicit surfaces $\sigma(\mathbf{r}) = 0$ and $\chi(\mathbf{r}) = 0$ intersect transversally in an irreducible curve $\gamma(\mathbf{r})$, then any algebraic surface $\eta(\mathbf{r}) = 0$ that meets $\sigma(\mathbf{r}) = 0$ with G^k rescaling continuity on $\gamma(\mathbf{r})$ must be in the form $\eta(\mathbf{r}) = \alpha(\mathbf{r})\sigma(\mathbf{r}) + \beta(\mathbf{r})\chi^{k+1}(\mathbf{r})$ where $\alpha(\mathbf{r})$ and $\beta(\mathbf{r})$ are polynomial functions that are not identically zero on $\gamma(\mathbf{r})$.

If considered in the standard unit domain $\mathbb{D}_0$ in Eqn.(3.6), the periodic grid surface that defines the domain boundary is

$$\chi_g(\mathbf{r}) = \cos\left(2\pi\kappa_g(\mathbf{e}_x^T \cdot \mathbf{r})\right)\cos\left(2\pi\kappa_g(\mathbf{e}_y^T \cdot \mathbf{r})\right)\cos\left(2\pi\kappa_g(\mathbf{e}_z^T \cdot \mathbf{r})\right)$$

where $\mathbf{e}_x = [1,0,0,-1/2]^T$, $\mathbf{e}_y = [0,1,0,-1/2]^T$, $\mathbf{e}_z = [0,0,1,-1/2]^T$, and $\kappa_g = 1/2$. It is rewritten in the generic form as

$$\chi_g(\mathbf{r}) = \sum_{i=1}^{4} \mu_g \cos\left(2\pi\kappa_g(\mathbf{e}_{gi}^T \cdot \mathbf{r})\right) \tag{3.7}$$

where $\mathbf{e}_{g1} = [1,1,1,-3/2]^T$, $\mathbf{e}_{g2} = [1,1,-1,-1/2]^T$, $\mathbf{e}_{g3} = [1,-1,1,-1/2]^T$, $\mathbf{e}_{g4} = [1,-1,-1,1/2]^T$, and $\mu_g = 1/4$.

Given a periodic surface $\psi(\mathbf{r}) = 0$, we can create a new surface $\psi^{(k)}(\mathbf{r}) = 0$ that meets with the original surface on the curve boundaries $\gamma(\mathbf{r}) = \psi^2(\mathbf{r}) + \chi_g^2(\mathbf{r}) = 0$ with G^k rescaling continuity as

$$\psi^{(k)}(\mathbf{r}) = \alpha(\mathbf{r})\psi(\mathbf{r}) + \beta(\mathbf{r})\chi_g^{k+1}(\mathbf{r}) \tag{3.8}$$

where $\alpha(\mathbf{r})$ and $\beta(\mathbf{r})$ satisfy the condition that $\exists \mathbf{r} \in \mathbb{D}_0, \gamma(\mathbf{r}) = 0, \alpha(\mathbf{r})\beta(\mathbf{r}) \neq 0$.

Example 4. An example of constrained degree elevation of P surface with G^0 continuity on the unit boundary is surface

$$\begin{aligned}\psi^{(0)}(x,y,z) = {} & \alpha\left\{\cos\left(2\pi(x)\right) + \cos\left(2\pi(y)\right) + \cos\left(2\pi(z)\right)\right\} \\ & +\beta\begin{Bmatrix} 0.25\cos\left(2\pi(0.5x+0.5y+0.5z-0.75)\right) + 0.25\cos\left(2\pi(0.5x+0.5y-0.5z-0.25)\right) \\ +0.25\cos\left(2\pi(0.5x-0.5y+0.5z-0.25)\right) + 0.25\cos\left(2\pi(0.5x-0.5y-0.5z+0.25)\right) \end{Bmatrix}\end{aligned}$$

An elevation with G^1 continuity results in surface

$$\begin{aligned}\psi^{(1)}(x,y,z) = {} & \alpha\left\{\cos\left(2\pi(x)\right) + \cos\left(2\pi(y)\right) + \cos\left(2\pi(z)\right)\right\} \\ & +\beta\begin{Bmatrix} 0.25\cos\left(2\pi(0.5x+0.5y+0.5z-0.75)\right) + 0.25\cos\left(2\pi(0.5x+0.5y-0.5z-0.25)\right) \\ +0.25\cos\left(2\pi(0.5x-0.5y+0.5z-0.25)\right) + 0.25\cos\left(2\pi(0.5x-0.5y-0.5z+0.25)\right) \end{Bmatrix}^2 \\ = {} & \alpha\left\{\cos\left(2\pi(x)\right) + \cos\left(2\pi(y)\right) + \cos\left(2\pi(z)\right)\right\} \\ & +\beta\begin{Bmatrix} 0.125 + 0.03125\cos\left(2\pi(x+y+z-1.5)\right) + 0.03125\cos\left(2\pi(x+y-z-0.5)\right) \\ +0.03125\cos\left(2\pi(x-y+z-0.5)\right) + 0.03125\cos\left(2\pi(x-y-z+0.5)\right) \\ +0.0625\cos\left(2\pi(x+y-1)\right) + 0.0625\cos\left(2\pi(x+z-1)\right) + 0.0625\cos\left(2\pi(y+z-1)\right) \\ +0.0625\cos\left(2\pi(x+0.5)\right) + 0.0625\cos\left(2\pi(z-0.5)\right) + 0.0625\cos\left(2\pi(y-0.5)\right) \\ +0.0625\cos\left(2\pi(x-0.5)\right) + 0.0625\cos\left(2\pi(y-z)\right) + 0.0625\cos\left(2\pi(x-z)\right) \\ +0.0625\cos\left(2\pi(y-0.5)\right) + 0.0625\cos\left(2\pi(x-y)\right) + 0.0625\cos\left(2\pi(z-0.5)\right) \end{Bmatrix}\end{aligned}$$

as compared in Fig. 8(a) and Fig. 8(b).

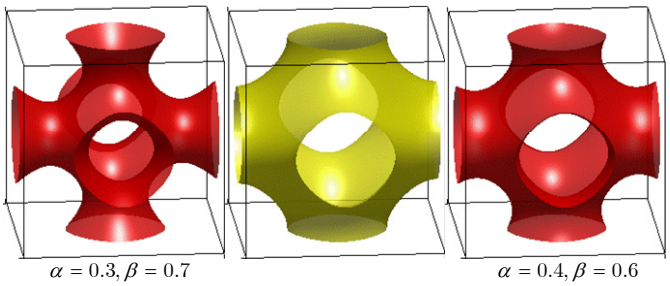

(a) G^0 continuity

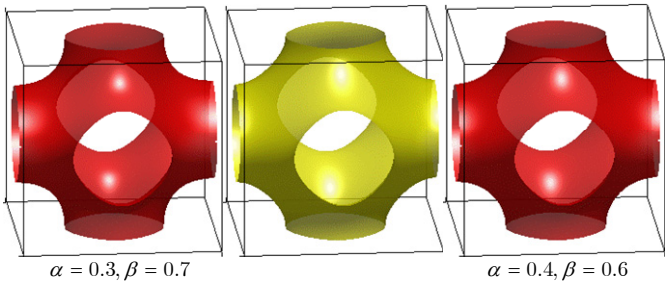

(b) G^1 continuity

Fig. 8: Examples of constrained degree elevation of P surface with G^0 and G^1 continuities, where yellow surfaces are the original P surfaces and red surfaces are the elevated ones.

Example 5. A polymer morphological model

$$\begin{aligned}\psi(x,y,z) = &-0.28087 + 0.32754\cos(2\pi x) + 0.34605\cos(2\pi y) - 0.29134\cos(2\pi z)\\ &- 0.15175\cos(2\pi(x+y)) + 0.44849\cos(2\pi(x+z)) - 0.043878\cos(2\pi(y+z))\\ &- 0.10382\cos(2\pi(x-y)) + 0.098657\cos(2\pi(z-x)) + 0.19572\cos(2\pi(y-z))\\ &- 0.16861\cos(2\pi(x+y+z)) - 0.28233\cos(2\pi(x-y+z))\\ &+ 0.15767\cos(2\pi(y+z-x)) - 0.16947\cos(2\pi(x+y-z))\\ &- 0.24857\cos(4\pi x) - 0.037011\cos(4\pi y) + 0.064369\cos(4\pi z)\\ &- 0.043344\cos(4\pi(x+y)) - 0.17759\cos(4\pi(x+z)) - 0.098227\cos(4\pi(y+z))\\ &+ 0.18506\cos(4\pi(x-y)) - 0.0018576\cos(4\pi(z-x)) + 0.074351\cos(4\pi(y-z))\\ &+ 0.086133\cos(4\pi(x+y+z)) - 0.056621\cos(4\pi(x-y+z))\\ &+ 0.030192\cos(4\pi(y+z-x)) + 0.029781\cos(4\pi(x+y-z))\\ = &\ 0\end{aligned}$$

as shown in Fig. 9(b) is elevated with boundary continuity constraints. Following Eqn.(3.8), we can construct two elevated PS models with G^0 and G^1 continuity as shown in Fig. 9(a) and Fig. 9(c) respectively.

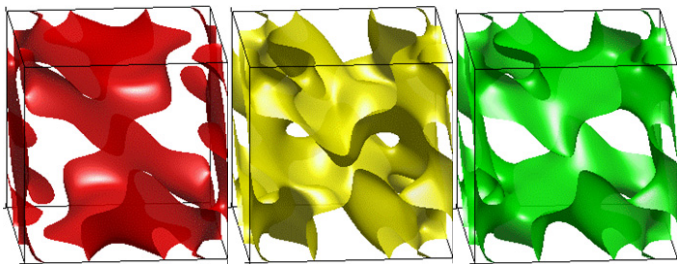

(a) G^0 continuity $\alpha = 0.1, \beta = 0.9$ (b) original polymer model (c) G^1 continuity $\alpha = 0.1, \beta = 0.9$

Fig. 9: A polymer PS model with constrained degree elevations.

4. DEGREE REDUCTION

For a surface in Eqn.(2.1), degree reduction in a domain $\mathbb{D}$ is to find a

$$\psi'(\mathbf{r}) = \sum_{l=1}^{L}\sum_{n=1}^{N} \mu'_{ln} \cos\left(2\pi\kappa_l(\mathbf{p}'^T_n \cdot \mathbf{r})\right)$$

where $N < M$ such that the *algebraic distance* between the two surfaces

$$\text{dist}(\psi, \psi') := \iiint_{\mathbb{D}} \left[\psi(\mathbf{r}) - \psi'(\mathbf{r})\right]^2 d\mathbf{r} \tag{4.1}$$

is minimized, where $\mathbb{D}$ is complete with respect to both ψ and ψ'. Eqn.(4.1) is rewritten as

$$\begin{aligned} \text{dist}(\psi, \psi') &= \left\langle \psi(\mathbf{r}) - \psi'(\mathbf{r}), \psi(\mathbf{r}) - \psi'(\mathbf{r}) \right\rangle \\ &= \sum_{l=1}^{L} \left\{ \begin{array}{l} \left\langle \sum_{m=1}^{M} \mu_{lm} \cos\left(2\pi\kappa_l(\mathbf{p}_m^T \cdot \mathbf{r})\right), \sum_{m=1}^{M} \mu_{lm} \cos\left(2\pi\kappa_l(\mathbf{p}_m^T \cdot \mathbf{r})\right) \right\rangle \\ -2\left\langle \sum_{m=1}^{M} \mu_{lm} \cos\left(2\pi\kappa_l(\mathbf{p}_m^T \cdot \mathbf{r})\right), \sum_{n=1}^{N} \mu'_{ln} \cos\left(2\pi\kappa_l(\mathbf{p}'^T_n \cdot \mathbf{r})\right) \right\rangle \\ +\left\langle \sum_{n=1}^{N} \mu'_{ln} \cos\left(2\pi\kappa_l(\mathbf{p}'^T_n \cdot \mathbf{r})\right), \sum_{n=1}^{N} \mu'_{ln} \cos\left(2\pi\kappa_l(\mathbf{p}'^T_n \cdot \mathbf{r})\right) \right\rangle \end{array} \right\} \end{aligned} \tag{4.2}$$

Given a new set of periodic vectors $\{\mathbf{p}'_n\}$, the goal of degree reduction is to find optimal moments $\{\mu'_{ln}\}$ so that the distance in Eqn.(4.2) is minimized. A necessary condition for the optimality is

$$\frac{\partial \,\text{dist}(\psi, \psi')}{\partial \mu'_{ln}} = 0 \quad (for\ l = 1, \ldots, L, n = 1, \ldots, N) \tag{4.3}$$

which is equivalent to

$$\begin{aligned} &2\mu'_{ln}\left\langle \cos\left(2\pi\kappa_l(\mathbf{p}'^T_n \cdot \mathbf{r})\right), \cos\left(2\pi\kappa_l(\mathbf{p}'^T_n \cdot \mathbf{r})\right)\right\rangle + 2\sum_{\substack{m=1 \\ m\neq n}}^{N} \mu'_{lm}\left\langle \cos\left(2\pi\kappa_l(\mathbf{p}'^T_m \cdot \mathbf{r})\right), \cos\left(2\pi\kappa_l(\mathbf{p}'^T_n \cdot \mathbf{r})\right)\right\rangle \\ &-2\sum_{m=1}^{M} \mu_{lm}\left\langle \cos\left(2\pi\kappa_l(\mathbf{p}_m^T \cdot \mathbf{r})\right), \cos\left(2\pi\kappa_l(\mathbf{p}'^T_n \cdot \mathbf{r})\right)\right\rangle = 0 \quad (for\ l = 1, \ldots, L, n = 1, \ldots, N) \end{aligned} \tag{4.4}$$

Thus, the problem of deriving optimal moments is reduced to solving L linear equation systems

$$[a_{lnm}]_{N\times N}[\mu'_{ln}]_{N\times 1} = [b_{ln}]_{N\times 1} \quad (for\ l = 1, \ldots, L) \tag{4.5}$$

where

$$a_{lnm} = \left\langle \cos\left(2\pi\kappa_l(\mathbf{p}'^T_m \cdot \mathbf{r})\right), \cos\left(2\pi\kappa_l(\mathbf{p}'^T_n \cdot \mathbf{r})\right)\right\rangle \tag{4.6}$$

and

$$b_{ln} = \sum_{m=1}^{M} \mu_{lm}\left\langle \cos\left(2\pi\kappa_l(\mathbf{p}_m^T \cdot \mathbf{r})\right), \cos\left(2\pi\kappa_l(\mathbf{p}'^T_n \cdot \mathbf{r})\right)\right\rangle \tag{4.7}$$

The computational complexity is mostly dependent on the numerical integral algorithms to compute the $LN(N+1)$ coefficients in Eqn.(4.6) and Eqn.(4.7).

Example 6. Surface

$$\begin{aligned}\psi_1(x,y,z) = &\cos\big(2\pi(-x+y+0.25)\big)+\cos\big(2\pi(-x-y+0.25)\big)+\cos\big(2\pi(-y+z+0.25)\big)\\ &+\cos\big(2\pi(-y-z+0.25)\big)+\cos\big(2\pi(x-z+0.25)\big)+\cos\big(2\pi(-x-z+0.25)\big)\\ &+0.5\cos\big(2\pi(5x)\big)+0.5\cos\big(2\pi(5y)\big)+0.5\cos\big(2\pi(5z)\big)\end{aligned}$$

which contains detailed features is reduced to a G-surface

$$\begin{aligned}\psi_{g1}(x,y,z) = &\cos\big(2\pi(-x+y+0.25)\big)+\cos\big(2\pi(-x-y+0.25)\big)+\cos\big(2\pi(-y+z+0.25)\big)\\ &+\cos\big(2\pi(-y-z+0.25)\big)+\cos\big(2\pi(x-z+0.25)\big)+\cos\big(2\pi(-x-z+0.25)\big)\end{aligned}$$

ψ_1 is the yellow surface in Fig. 10(a), and ψ_{g1} is the blue surface in Fig. 10(b).

Surface

$$\begin{aligned}\psi_2(x,y,z) = &\cos\big(2\pi(-x+y+0.25)\big)+\cos\big(2\pi(-x-y+0.25)\big)+\cos\big(2\pi(-y+z+0.25)\big)\\ &+\cos\big(2\pi(-y-z+0.25)\big)+\cos\big(2\pi(x-z+0.25)\big)+\cos\big(2\pi(-x-z+0.25)\big)\\ &+\cos\big(2\pi(1.3x-1.7y)\big)+\cos\big(2\pi(0.3y)\big)+\cos\big(2\pi(1.3z)\big)\end{aligned}$$

is also reduced to a G-surface

$$\begin{aligned}\psi_{g2}(x,y,z) = &1.0387\cos\big(2\pi(-x+y+0.25)\big)+1.2902\cos\big(2\pi(-x-y+0.25)\big)\\ &+\cos\big(2\pi(-y+z+0.25)\big)+\cos\big(2\pi(-y-z+0.25)\big)+\cos\big(2\pi(x-z+0.25)\big)\\ &+\cos\big(2\pi(-x-z+0.25)\big)\end{aligned}$$

ψ_2 is the yellow surface in Fig. 11(a), and ψ_{g2} is the blue surface in Fig. 11(b).

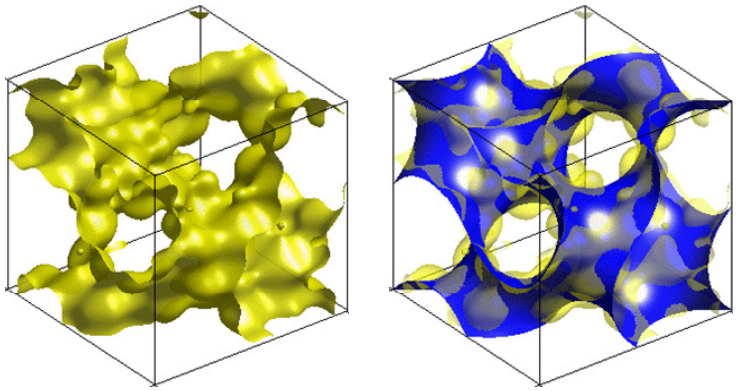

(a) original surface (b) reduced surface

Fig. 10: Degree reduction of surface ψ_1 where the original surface is in yellow and the reduced G-surface is in blue.

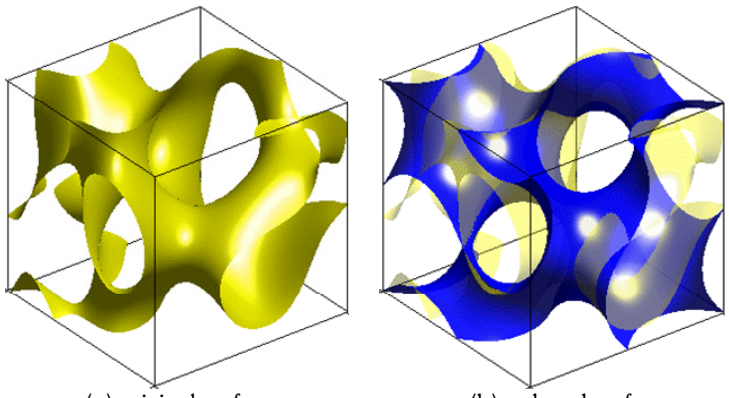

(a) original surface (b) reduced surface

Fig. 11: Degree reduction of surface ψ_2 where the original surface is in yellow and the reduced G-surface is in blue.

Lemma 3. Based on the algebraic distance in Eqn.(4.1), if the set of the new basis vectors $\{\mathbf{p}'_n\}$ is a subset of the original vectors $\{\mathbf{p}_m\}$, i.e., $\mathbf{p}'_n = \mathbf{p}_n$ $(n = 1,\ldots,N)$, and the basis vectors $\{\mathbf{p}_m\}$ are orthogonal to each other at the same scale in a domain $\mathbb{D}$, then degree reduction in $\mathbb{D}$ is simply to extract the corresponding subset of moments $\mu'_n = \mu_n$ $(n = 1,\ldots,N)$.

Proof. From Eqn.(4.6), because of the assumed orthogonality, for any given scale l, we have $a_{lnm} = \begin{cases} 0 & (if\ m \neq n) \\ \left\langle \cos\left(2\pi\kappa_l(\mathbf{p}'^T_n \cdot \mathbf{r})\right), \cos\left(2\pi\kappa_l(\mathbf{p}'^T_n \cdot \mathbf{r})\right)\right\rangle & (if\ m = n) \end{cases}$. Similarly, from Eqn.(4.7), we have $b_{ln} = \mu_{ln}\left\langle \cos\left(2\pi\kappa_l(\mathbf{p}'^T_n \cdot \mathbf{r})\right), \cos\left(2\pi\kappa_l(\mathbf{p}'^T_n \cdot \mathbf{r})\right)\right\rangle$. Solving Eqn.(4.5), we can easily derive $\mu'_{ln} = \mu_{ln}$ $(n = 1,\ldots,N)$.

□

Lemma 3 ensures the simplicity of degree reduction for the special case. Suppose there are K pairs of moments and periodic vectors that are common for ψ and ψ', that is, $\mu_{lm} = \mu'_{lm}$ and $\mathbf{p}_m = \mathbf{p}'_m$ for all $l = 1,\ldots,L$ and $m = 1,\ldots,K$. It is easy to verify that

$$\sum_{l=1}^{L}\left\{\begin{array}{l} \left\langle \sum_{m=1}^{K}\mu_{lm}\cos\left(2\pi\kappa_l(\mathbf{p}_m^T\cdot\mathbf{r})\right), \sum_{m=1}^{K}\mu_{lm}\cos\left(2\pi\kappa_l(\mathbf{p}_m^T\cdot\mathbf{r})\right)\right\rangle \\ -2\left\langle \sum_{m=1}^{K}\mu_{lm}\cos\left(2\pi\kappa_l(\mathbf{p}_m^T\cdot\mathbf{r})\right), \sum_{n=1}^{K}\mu'_{ln}\cos\left(2\pi\kappa_l(\mathbf{p}'^T_n\cdot\mathbf{r})\right)\right\rangle \\ +\left\langle \sum_{n=1}^{K}\mu'_{ln}\cos\left(2\pi\kappa_l(\mathbf{p}'^T_n\cdot\mathbf{r})\right), \sum_{n=1}^{K}\mu'_{ln}\cos\left(2\pi\kappa_l(\mathbf{p}'^T_n\cdot\mathbf{r})\right)\right\rangle \end{array}\right\} = 0$$

Thus only those components that are different in either moments or periodic vectors in two surface models contribute to the algebraic distance.

$$\mathrm{dist}(\psi,\psi') = \sum_{l=1}^{L}\left\{\begin{array}{l} \left\langle \sum_{m=K+1}^{M}\mu_{lm}\cos\left(2\pi\kappa_l(\mathbf{p}_m^T\cdot\mathbf{r})\right), \sum_{m=K+1}^{M}\mu_{lm}\cos\left(2\pi\kappa_l(\mathbf{p}_m^T\cdot\mathbf{r})\right)\right\rangle \\ -2\left\langle \sum_{m=K+1}^{M}\mu_{lm}\cos\left(2\pi\kappa_l(\mathbf{p}_m^T\cdot\mathbf{r})\right), \sum_{n=K+1}^{N}\mu'_{ln}\cos\left(2\pi\kappa_l(\mathbf{p}'^T_n\cdot\mathbf{r})\right)\right\rangle \\ +\left\langle \sum_{n=K+1}^{N}\mu'_{ln}\cos\left(2\pi\kappa_l(\mathbf{p}'^T_n\cdot\mathbf{r})\right), \sum_{n=K+1}^{N}\mu'_{ln}\cos\left(2\pi\kappa_l(\mathbf{p}'^T_n\cdot\mathbf{r})\right)\right\rangle \end{array}\right\} \quad (4.8)$$

In particular, if all pairs of basis vectors are identical but the corresponding moments are different, that is, $\mathbf{p}_m = \mathbf{p}'_m$ and $\mu_{lm} \neq \mu'_{lm}$ for all $l = 1,\ldots,L$ and $m = K+1,\ldots,M$, then the distance in Eqn.(4.8) is reduced to

$$\mathrm{dist}_{\parallel}(\psi,\psi') = \sum_{l=1}^{L}\sum_{m=K+1}^{M}(\mu_{lm}-\mu'_{lm})^2\left\langle\cos\left(2\pi\kappa_l(\mathbf{p}_m^T\cdot\mathbf{r})\right),\cos\left(2\pi\kappa_l(\mathbf{p}_m^T\cdot\mathbf{r})\right)\right\rangle$$

If basis vectors $\mathbf{p}_m$'s and $\mathbf{p}'_n$'s are all orthogonal to each other at every scale l in $\mathbb{D}$, then Eqn.(4.8) is reduced to

$$\mathrm{dist}_{\perp}(\psi,\psi') = \sum_{l=1}^{L}\left\{\begin{array}{l}\displaystyle\sum_{m=K+1}^{M}\mu_{lm}^2\left\langle\cos\left(2\pi\kappa_l(\mathbf{p}_m^T\cdot\mathbf{r})\right),\cos\left(2\pi\kappa_l(\mathbf{p}_m^T\cdot\mathbf{r})\right)\right\rangle \\ \displaystyle+\sum_{n=K+1}^{N}\mu'^2_{ln}\left\langle\cos\left(2\pi\kappa_l(\mathbf{p}'^T_n\cdot\mathbf{r})\right),\cos\left(2\pi\kappa_l(\mathbf{p}'^T_n\cdot\mathbf{r})\right)\right\rangle\end{array}\right\}$$

5. CONCLUDING REMARKS

Degree elevation and reduction operations are two basic mechanisms to control the complexity of surface models in multi-resolution representations. In this paper, we study degree operations of periodic surfaces. Three degree elevation approaches are developed, including native degree elevation that is scale independent and without modifying existing basis vectors; scale-dependent variational degree elevation which modifies existing basis vectors; and constrained degree elevation with boundary continuity conditions which supports piecewise construction and assembly. A generic degree reduction method is also developed based on an algebraic distance measurement. The study is to seek the extension of the traditional degree operation concept in surface modeling to periodic surfaces for nano-scale geometric design.

6. ACKNOWLEDGEMENTS

This work is supported in part by the NSF Grant CMMI-0645070.

7. REFERENCES

[1] Wang, Y.: Geometric modeling of nano structures with periodic surfaces, Proc. GMP2006, Pittsburgh, PA, July 26-28, In Lecture Notes in Computer Science, ed. by M.-S. Kim and K. Shimada, 4077, 2006, 343-356.
[2] Wang, Y: Periodic surface modeling for computer aided nano design, Computer-Aided Design, 39(3), 2007, 179-189.
[3] Wang, Y: Loci periodic surface reconstruction from crystals, Computer-Aided Design & Applications, 4(1-4), 2007, 437-447.
[4] Bloomenthal, J.: Introduction to implicit surfaces. Morgan Kaufmann, San Francisco, CA, 1997.
[5] Blinn, J.F.: A generalization of algebraic surface drawing, ACM Trans. Graphics, 1(3), 1982, 235-256.
[6] Muraki, S.: Volumetric shape description of range data using "blobby model", Computer Graphics, 25(4), 1991, 227-235.
[7] Bloomenthal, J.; Shoemake, K.: Convolution surfaces, Computer Graphics, 25(4), 1991, 251-256.
[8] Sederberg, T.W.: Surfaces: Techniques for cubic algebraic surfaces, IEEE CG&A, 10(4), 1991, 14-25.
[9] Sederberg, T.W.; Anderson, D.C.; Goldman, R.N.: Implicit representation of parametric curves and surfaces, Computer Vision, Graphics, & Image Processing, 28(1), 1984, 72-84.
[10] Hoffmann, C.M.: Implicit curves and surfaces in CAGD, IEEE Computer Graphics & Applications, 16(3), 1993, 245-254.
[11] Sederberg, T.W.; Saito, T.; Qi, D.; Klimaszewski, K.S.: Curve implicitization using moving lines, Computer Aided Geometric Design, 11(6), 1994, 687-706.
[12] Berry, T.G.; Patterson, R.R.: Implicitization and parametrization of nonsingular cubic surfaces, Computer Aided Geometric Design, 18, 2001, 723-738.
[13] Chen, F.; Sederberg, T.: A new implicit representation of a planar rational curve with high order singularity. Computer Aided Geometric Design, 19, 2002, 151-167.
[14] Hoffmann, C.; Hopcroft, J.: Quadric blending surfaces, Computer-Aided Design, 18, 1986, 301-306.
[15] Warren, J.: Blending algebraic surfaces, ACM Trans. Graphics, 8(4), 1989, 263-278.
[16] Hartmann, E.: Blending an implicit with a parametric surface, Computer Aided Geometric Design, 12(8), 1995, 825-835.

[17] Wu, T.-R.; Zhou, Y.-S.: On blending of several quadratic algebraic surfaces, Computer Aided Geometric Design, 17, 2000, 759-766.
[18] Hartmann, E.: Implicit G^n-blending of vertices, Computer Aided Geometric Design, 18, 2001, 267-285.
[19] Bajaj, C.; Ihm, I.; Warren, J.: High-order interpolation and least-squares approximation using implicit algebraic surfaces, ACM Trans. Graphics, 12(4), 1993, 327-347.
[20] Turk, G.; O'brien, J.F.: Modelling with implicit surfaces that interpolate, ACM Trans. Graphics, 21(4), 2002, 855-873.
[21] Sederberg, T.: Piecewise algebraic surface patches, Computer Aided Geometric Design, 2(1-3), 1985, 53-60.
[22] Witkin, A.P.; Heckbert, P.S.: Using particles to sample and control implicit surfaces. Proc. SIGGRAPH'94, 1994, pp.269-277.
[23] Goldman, R.: Curvature formulas for implicit curves and surfaces, Computer Aided Geometric Design, 22(7), 2005, 623-658.
[24] Zhang, Q.; Xu, G.: Curvature computations for n-manifolds in R^{n+m} and solution to an open problem proposed by R. Goldman, Computer Aided Geometric Design, 24, 2007, 117-123.
[25] Che, W.; Paul, J.-C.; Zhang, X.: Lines of curvature and umbilical points for implicit surfaces, Computer Aided Geometric Design, 24, 2007, 395-409.
[26] Wyvill, G.; McPheeters, C.; Wyvill, B.: Data structure for soft objects, The Visual Computer, 2(2), 1986, 227-234.
[27] Lorensen, W.E.; Cline, H.E.: Marching cubes: A high resolution 3D surface construction algorithm, Computer Graphics, 21(4), 1987, 163-169.
[28] Bloomenthal, J.: Polygonization of implicit surfaces, Computer Aided Geometric Design, 5(4), 1988, 341-355.
[29] Kalra, D.; Barr, A.H.: Guaranteed ray intersections with implicit surfaces, Computer Graphics, 23(3), 1989, 297-306.
[30] Hart, J.: Sphere tracing: a geometric method for the antialiased ray tracing of implicit surfaces, The Visual Computer, 12(10), 1996, 527-545.
[31] Connolly, M.L.: Molecular Surfaces: A Review, Network Science, 1996, http://www.netsci.org/Science/Compchem/index.html
[32] Lee, B.; Richards, F.M.: The interpretation of protein structures: Estimation of static accessibility. Journal of Molecular Biology, 55(3), 1971, 379-400.
[33] Connolly, M.L.: Solvent-accessible surfaces of proteins and nucleic acids, Science, 221(4612), 1983, 709-713.
[34] Carson, M: Wavelets and molecular structure, Journal of Computer Aided Molecular Design, 10(4), 1996, 273-283.
[35] Edelsbrunner, H.: Deformable smooth surface design, Discrete & Computational Geometry, 21(1), 1999, 87-115.
[36] Bajaj, C.; Pascucci, V.; Shamir, A.; Holt, R.; Netravali, A.: Dynamic maintenance and visualization of molecular surfaces, Discrete Applied Mathematics, 127(1), 2003, 23-51.
[37] Au, C.K.; Woo, T.C.: Ribbons: their geometry and topology, Computer-Aided Design & Applications, 1(1-4), 2004, 1-6.
[38] Ryu, J.; Kim, D.; Cho, Y.; Park, R.; Kim, D.-S.: Computation of molecular surface using Euclidean Voronoi Diagram, Computer-Aided Design & Applications, 2(1-4), 2005, 439-448.
[39] Zhang, Y.; Xu, G; Bajaj, C: Quality meshing of implicit solvation models of biomolecular structures, Computer-Aided Geometric Design, 23(6), 2006, 510-530.